Proceedings of the ASME 2010 3rd Joint US-European Fluids Engineering Summer Meeting and 8th International Conference on Nanochannels, Microchannels, and Minichannels
FEDSM-ICNMM2010
August 1-5, 2010, Montreal, Canada

FEDSM-ICNMM2010-30923

Theoretical Stability Analysis of Self-Excited Vibration in a Thin Film Wrapped around an Air-Turn Bar

Masahiro WATANABE and Kensuke HARA
Department of Mechanical Engineering,
Aoyama Gakuin University
5-10-1, Fuchinobe, Sagamihara-shi, Kanagawa, 229-8558, Japan

ABSTRACT

This paper deals with a theoretical stability analysis of a self-excited vibration generated in a film wrapped around an air-turn bar. In this paper, firstly, vibration characteristics of the self-excited vibration are examined experimentally, and it is shown that two different types of self-excited vibration, which are low-frequency and high-frequency modes, occur in the film. Secondly, stability of the low-frequency mode is examined theoretically. A theoretical model of the film wrapped around the air-turn bar is developed. Basic equations of the air flow in the gap between the film and air-turn bar, and pressurized air flow inside the air-turn bar are derived. The characteristics equation of the system is derived from the basic equations of motion of the film coupled with the air flow. Instability condition in which the self-excited vibration occurs is shown as a function of air flow rate and tension applied to the film. Moreover, instability mechanism of the self-excited vibration is discussed based on the theoretical model.

NOMENCLATURE

B : Film width in cross direction [m] = Slit length [m]
d : Slit width [m]
H : Gap width between the film and air-turn bar [m]
$\overline{H}$, ΔH : Steady and unsteady components of H
K : Volume elasticity modulus [Pa]
P : Pressure in the air-turn bar [Pa]
$\overline{P}$, ΔP : Steady and unsteady components P
P_c : Pressure at the slit [Pa]
$\overline{P}_c$, ΔP_c : Steady and unsteady components of P_c
P_g : Pressure in the gap [Pa]
$\overline{P}_g$, ΔP_g : Steady and unsteady components of P_g
Q : Flow rate injected from the slit [m^3/s]
$\overline{Q}$, ΔQ : Steady and unsteady components of Q
Q_g : Flow rate per unit width in the gap [m^2/s]
$\overline{Q}_g$, ΔQ_g : Steady and unsteady components of Q_g
Q_s : Flow rate supplied to the air-turn bar [m^3/s]
R : Radius of the air-turn bar [m]
T : Tension per unit length [N/m]
$\overline{T}$, ΔT : Steady and unsteady components of T
V : Inner volume of the air-turn bar [m^3]
γ : Polytropic index
Θ : Wrapped angle of the film [rad.]
λ : Friction coefficient
ρ : Air density [kg/m^3]
τ : Time constant [sec]

INTRODUCTION

Air-turn bars with air emitting holes or slits are widely used for non-contact supporting and feeding of films in production processes of functional thin film. An air cushion is formed in the gap between the film and the air-turn bar by injecting pressurized air through the holes or slits. The film floats over the air cushion and the feeding direction of the film is thus changed without contacting the air-turn bar. One of the problems with respect to this device is a vibration generated in the film wrapped around the air-turn bar. In manufacturing fields of functional plastic thin films, it was reported that self-excited vibrations, which cause damage by scratching, occur in the film wrapped around the air-turn bar. Therefore, it is important to clarify the instability condition in which the self-excited vibration occurs in the film wrapped around the air-turn bar to avoid the damage.

Up to this time, some research works were conduced with respect to a web wrapped around an air-turn bar and

 Copyright © 2010 by ASME

cylindrical guides [1]-[8]. Muftu et al. presented a theoretical model of a web wrapped around an air-turn bar with air-emitting holes and analyzed the deflection of web and pressure distribution on the air-turn bar [1]-[3]. Chang and Moretti studied aerodynamic characteristics of pressure-pad air bars [4]. Hashimoto analyzed the air film thickness and friction characteristics on stationary guides in web handling processes [5]-[7]. On the other hand, many research works were conducted with respect to flutter generated in flexible sheet and web subjected to axial air flow [8]-[24]. However, vibration characteristics and instability condition of the self-excited vibration generated in the film wrapped around the air-turn bar are not clarified.

In the present work, firstly, vibration characteristics of the self-excited vibration generated in a film wrapped around the air-turn bar are examined experimentally. Then, it is shown that two different types of self-excited vibration, which are low-frequency and high-frequency modes, occur in the film. Secondly, a theoretical model of the film, which is wrapped around the air-turn bar, is supported on the pressurized air cushion formed around the air-turn bar, is developed and stability of the self-excited vibration in the film is examined theoretically. In particular, in the present paper, stability analysis with respect to the low-frequency mode, in which the film vibrates in the out-of-plane direction on the pressurized air cushion, is conducted. Stability diagram of the system and instability condition of the self-excited vibration are indicated as a function of air flow rate and tension applied to the film. Moreover, instability mechanism of the self-excited vibration is discussed based on the theoretical model.

EXPERIMENT

Experimental Setup

A schematic diagram and a photograph of the experimental setup are shown in Figure 1 and Figure 2, respectively. A test air-turn bar with an air supply slit is shown in Figure 3, and the major dimensions of the test air-turn bar are shown in Table 1. Measurement system for pressure fluctuation around and inside the air-turn bar is shown in Figure 4.

An air cushion is formed in the gap between the film and air-turn bar by injecting pressurized air through the slit. The film floats over the air cushion on the air-turn bar. In the experimental setup, the test film #1 is wrapped around the air-turn bar #2 and supported by four guide rollers #3. The film is 16 μm in thickness and 450 mm in width, and material of the film is PET (Polyethylene Terephthalate). Tension is applied to the film by using weights #4 set at both ends of the film. The wrapped angle of the film on the air-turn bar is 90 degrees. Air is supplied to the air-turn bar by using a blower #8 through a flexible pipe, and air flow rate is measured by a flow meter #7 set at the air supply pipe.

The vibration displacement of the film is measured by using three laser-displacement sensors #5 at Point-A, -B and -C, with changing the air flow rate and tension. Pressure fluctuation inside the air-turn bar and in the gap between the film and air-turn bar are measured by using pressure sensors, as shown in Figure 4. Moreover, sound pressure around the vibrating film is measured by pressure sensors #6 at Point-D and -E.

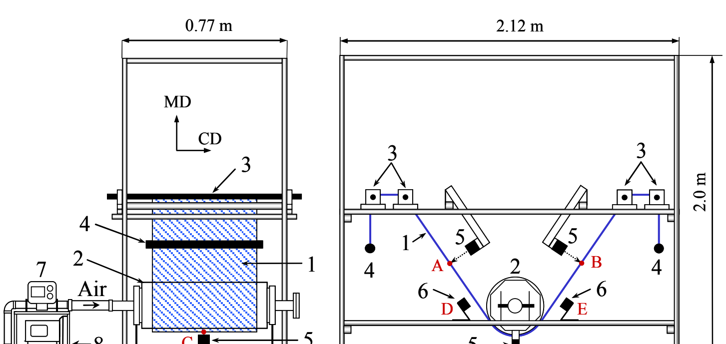

1 Film, 2 Air-turn bar, 3 Guide roller, 4 Weight, 5 Laser displacement sensor, 6 (Sound) Pressure sensor, 7 Flow meter, 8 Blower

Figure 1 Schematic diagram of the experimental setup

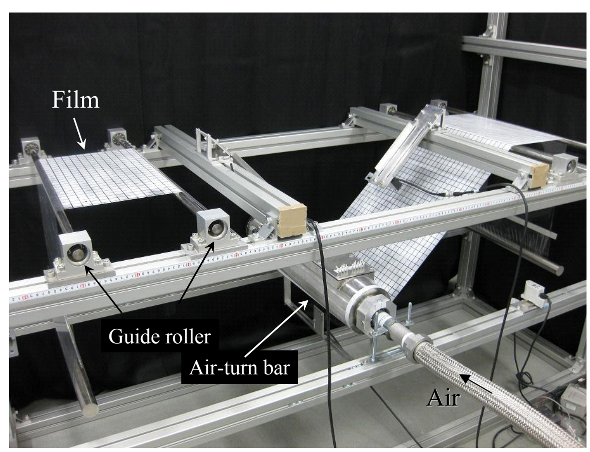

Figure 2 Photograph of the experimental setup

Copyright © 2010 by ASME

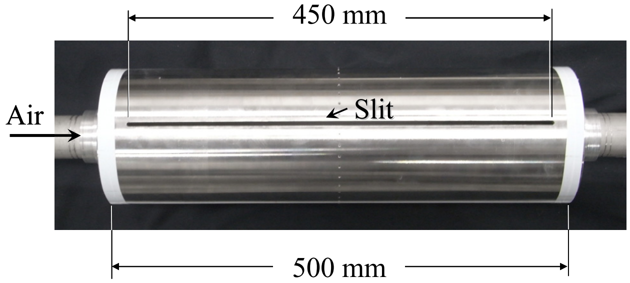

Figure 3 Test air-turn bar with an air supply slit

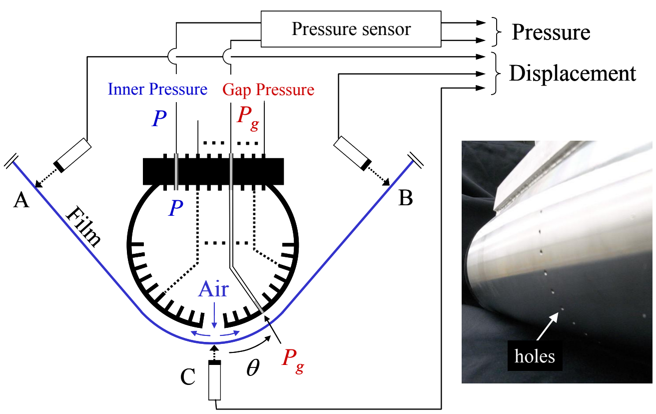

Figure 4 Schematic diagram of pressure measurement system.

Table 1 Major dimensions of the test air-turn bar

Diameter	Length	Slit width	Slit length
100 mm	500 mm	3 mm	450 mm

Experimental Results

Figure 5 and Figure 6 show the variation of the vibration displacement of the film and sound pressure around the film with increasing flow rate, respectively. Typical time histories and its spectrum at flow rate Q_1 and Q_2 are shown in Figure 7 and Figure 8. It can be seen that two different types of the self-excited vibration occur in the film.

The one is the high-frequency mode which occurs in Region-I. Its vibration mode is shown in Figure 9(a), in which the film vibrates violently at the end of wrapped area with buzz. The displacement of this type vibration is small, but its frequency is very high, so that large sound generates around the film. The mode shape of the high-frequency vibration was not clarified in this study, but it was found that the high-frequency vibration mode is very sensitive to the diameter of the air-turn bar, tension and air flow rate. The high-frequency vibration mode changes to another one, which has different high frequency, by changing the above parameters.

The other is the low-frequency mode which occurs in Region-II. Its vibration mode is shown in Figure 9(b), in which the film vibrates on the pressurized air cushion in the out-of-plane direction at Point-C. The frequency of this type vibration is low, and the out-of-plane displacement at Point-C is large, but the vibration displacements at Point-A and -B are small. In-plane sliding motion occurs in the film between the air-turn bar and guide roller, and between the guide rollers. Moreover, in the higher flow rate region (Region-III), large vibration occurs not only at Point-C but also at Point-A and -B. In this region, complex vibration occurs in the film with many dominant frequencies.

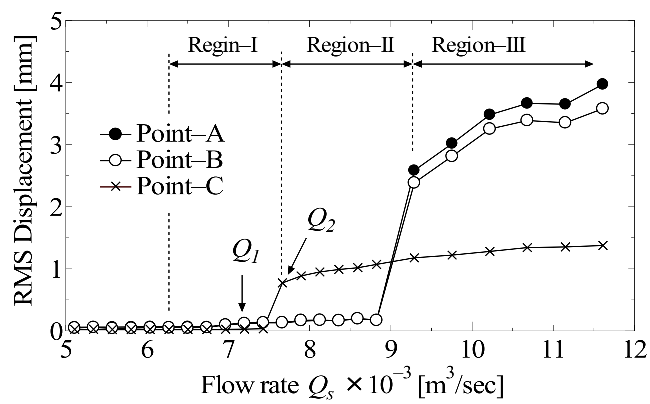

Figure 5 RMS vibration displacement with increasing flow rate for $T = 110$ N/m

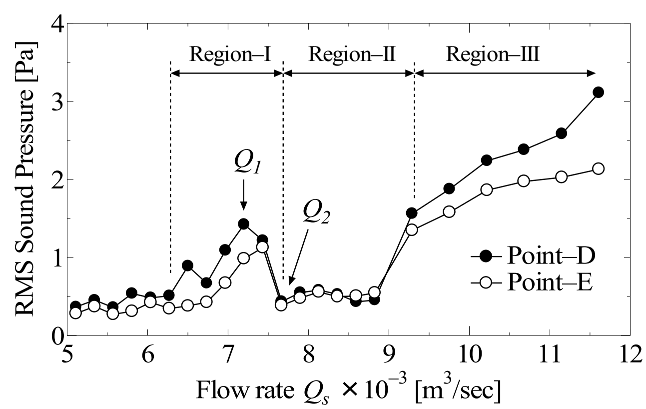

Figure 6 RMS sound pressure with increasing flow rate for $T = 110$ N/m

Copyright © 2010 by ASME

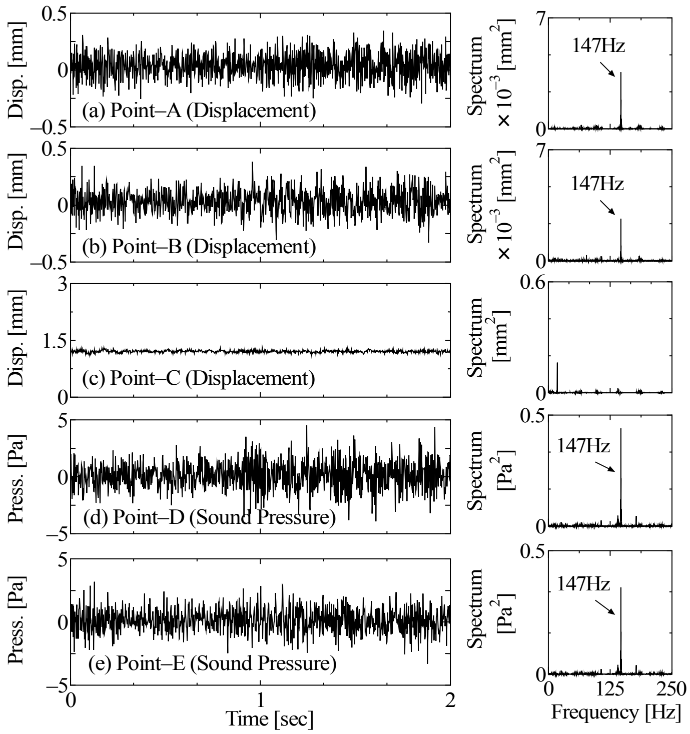

Figure 7 Time histories of vibration displacement and sound pressure for $Q_1 = 7.20 \times 10^{-3}$ m^3/s, $T = 110$ N/m

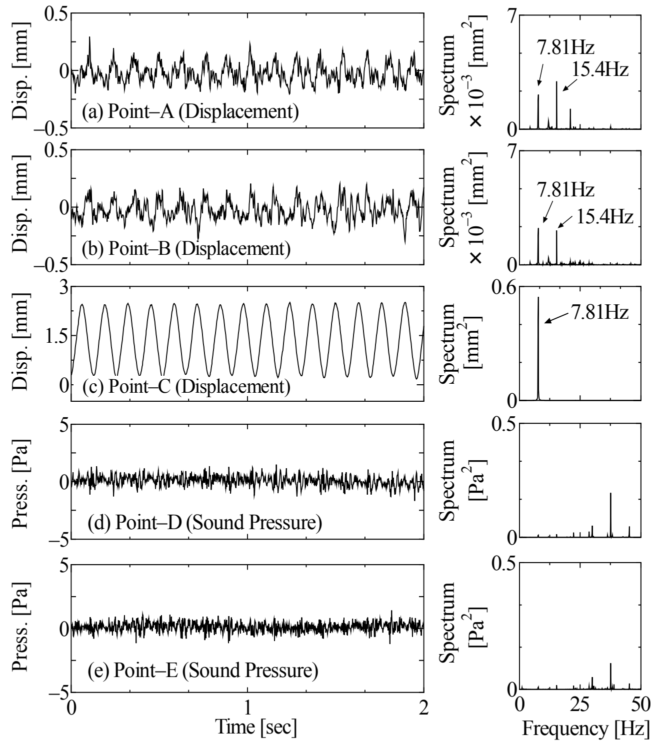

Figure 8 Time histories of vibration displacement and sound pressure for $Q_2 = 7.67 \times 10^{-3}$ m^3/s, $T = 110$ N/m

Figure 10 shows magnitude of the pressure fluctuation in the gap between the air-turn bar and film, in Region-II, when the low-frequency mode vibration occurs in the film. It can be seen that the air pressure oscillates over the broad area in the wrapped region (wrapped angle $-45 < \theta < 45$ degrees). In the outside of the wrapped area, there is no pressure fluctuation on the air-turn bar.

Figure 11(a) and (b) show the time histories of pressure fluctuation in the gap and air-turn bar, respectively, when the low-frequency mode vibration occurs in the film. The vibration displacement of the film at Point-C is also shown in these figures by broken line. It is seen that the air pressure oscillates not only in the gap but also inside the air-turn bar. From the Lissajous curves as shown in Figure 11, it is seen that the air pressure varies coupled with the film vibration, and phase of the pressure fluctuation is led, $+160 \sim +180$ degrees, against the vibration displacement of the film. Therefore, it is found that the self-excited vibration occurs in the film due to the air pressure fluctuation which is coupled with the film vibration.

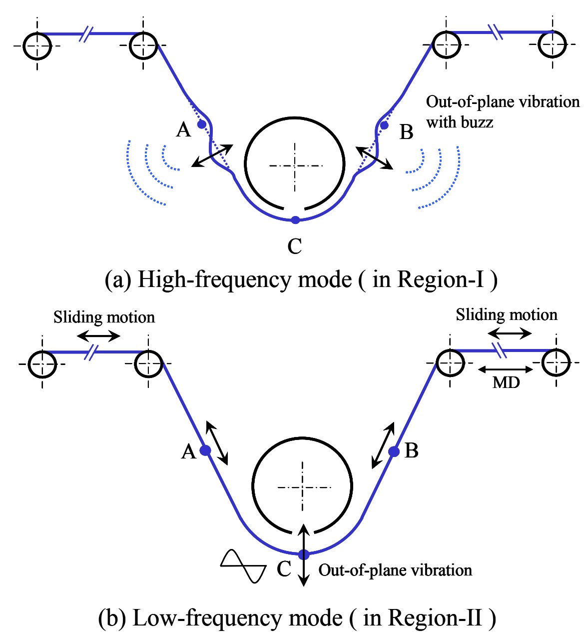

Figure 9 Vibration modes of the film

Copyright © 2010 by ASME

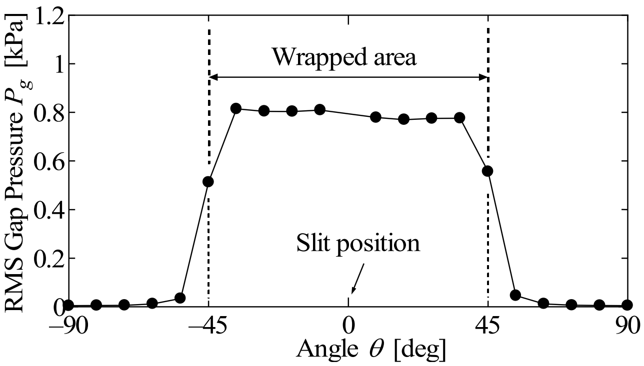

Figure 10 RMS pressure fluctuation in the gap when the low-frequency mode vibration occurs

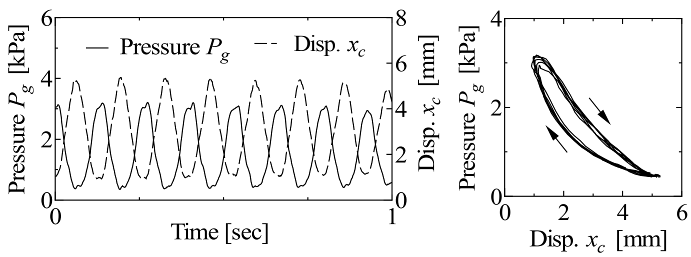

(a) Pressure fluctuation in the gap between the film and air-turn bar

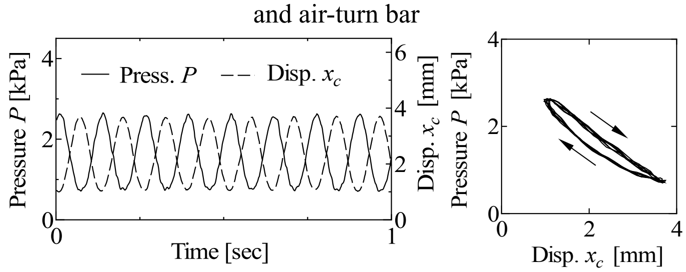

(b) Pressure fluctuation in the air-turn bar

Figure 11 Time histories and Lissajous curves of pressure fluctuation and vibration displacement at Point-C

THEORETICAL STABILITY ANALYSIS FOR THE LOW -FREQUENCY VIBRATION MODE

Analytical Model and Assumptions

In this study, theoretical stability analysis for the low-frequency mode vibration, which is shown above in the experimental results, is conducted. Figure 12 shows an analytical model of the system with a coordinate system. A film is wrapped around an air-turn bar which has a slit in the center and supported by guide rollers. Tension is applied to the film in the axial direction. Air cushion is formed in the gap between the film and air-turn bar by injecting pressurized air through the slit. The film floats over the air cushion on the air-turn bar. The dynamic characteristics of tension control in the film by PID control are modeled by equivalent spring-mass systems at the both ends of the film.

In order to simplify the analytical model while not losing important factors relevant to the instability phenomena, the following assumptions are made with respect to the interaction between the film and air flow. (1) Air in the gap flows only in the circumferential direction, and assumed does not flow axially along the air-turn bar. (2) In the wrapped area on the air-turn bar, the equilibrium gap width and the amplitude of the film vibration are constant in the circumference direction. (3) The effect of the feeding of the film in the circumferential direction can be neglected, because the feeding speed is much smaller that the air flow speed in the gap. (4) The effect of the bending stiffness of the film can be neglected against the tension.

Basic Equations of the Air Flow

Basic equations of the air flow in the gap between the film and air-turn bar can be written as follow:

$$Q(t) = 2BQ_g(t)\,, \tag{1}$$

$$\frac{dP_g(x,t)}{dx} = -\rho \frac{\lambda}{4} \frac{Q_g^2(t)}{H^3(t)}\,, \tag{2}$$

where $Q(t)$ is air flow rate supplied through the silt, $Q_g(t)$ is air flow rate per unit width in the gap in the cross direction. B is slit length which is equal to the film width. $P_g(x,t)$ is air pressure in the gap, and $H(t)$ is gap width. λ is coefficient of wall friction and is given by [25],

$$\lambda = 0.266\,\mathrm{Re}^{-0.25} \quad \text{for } \mathrm{Re} > 10^3\,, \tag{3}$$

where Re is Reynolds number of air flow in the gap and is defined as $\mathrm{Re} = Q_g / \nu$, and $\nu = \mu / \rho$.

The boundary conditions of the air flow in the gap can be written as follows:

$$P_g(0,t) = P_c(t) \quad \text{for } x = 0\,, \tag{4}$$

$$P_g(L,t) = P_a = 0 \ \text{ for } x = L = \frac{\Theta}{2} R\,, \tag{5}$$

where P_a is atmospheric pressure, which is defined as a reference pressure, and $P_c(t)$ is pressure at the slit and is given as follows.

If the silt width d is large, the pressure loss at the slit is neglected, so that the following equation is used for the boundary condition at the slit with respect to pressure $P_c(t)$,

$$P_c(t) = P(t)\,, \tag{6}$$

 Copyright © 2010 by ASME

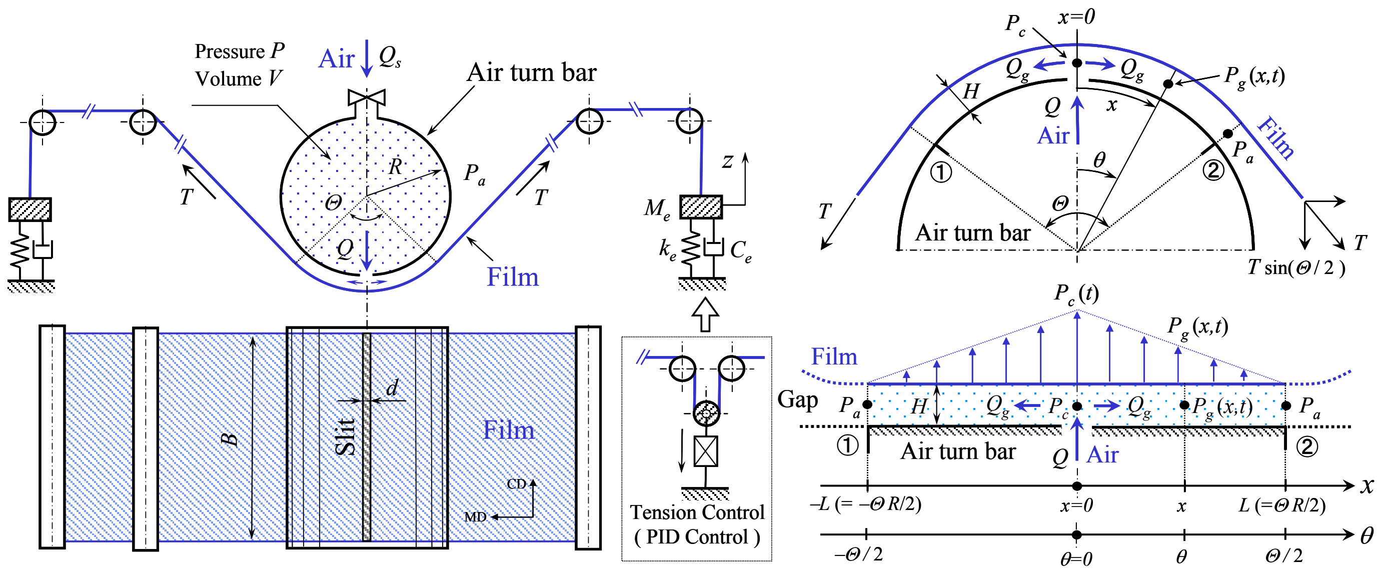

Figure 12 Theoretical model of the film wrapped around the air-turn bar

where $P(t)$ is the air pressure inside the air-turn bar. On the other hand, if the slit width d is small, the pressure loss is not negligible, so that the following equation is used for the boundary condition at the silt with respect to the flow rate $Q(t)$,

$$Q = C_d A_e \sqrt{2(P - P_c)/\rho}\ , \tag{7}$$

where C_d and $A_e = Bd$ are flow rate coefficient and area of the slit, respectively. ρ is air density.

In the present analysis, Equation (6) is used for the boundary condition at the slit, because the slit width of the test air-turn bar is 3 mm, which is sufficiently large against the equilibrium gap width between the film and air-turn bar.

Substituting Equations (4) and (5) of the boundary condition into Equation (2), the gap pressure and the pressure at the slit can be obtained as follows:

$$P_g(x,t) = P_c(t)(1 - \frac{x}{L})\ , \tag{8}$$

$$P_c(t) = \rho \frac{\lambda L}{4} \frac{Q_g^2(t)}{H^3(t)}\ . \tag{9}$$

Considering compressibility of air in the air-turn bar, the continuity equation of the air flow is written as follows:

$$\frac{V}{K}\frac{dP(t)}{dt} = Q_s - Q(t)\ , \tag{10}$$

where K is volume elasticity modulus of air in the air-turn bar and is given by $K = \gamma \overline{P}$ using Polytropic index γ. Q_s and $Q(t)$ are flow rate supplied to the air-turn bar and ejected through the slit, respectively. V is volume of air inside the air-turn bar

Basic Equations of the Film Motion

Force balance equation with respect to the tension applied to the film and air pressure in the gap are given by

$$T(t)\sin\frac{\Theta}{2} = \int_0^L (P_g(x,t) - P_a)\cos\theta\, dx\ . \tag{11}$$

where Θ is wrapped angle of the film on the air-turn bar. Equation (11) leads the following simplified equation.

$$T(t) = \alpha R P_c(t)\ , \tag{12}$$

$$\alpha = (1 - \cos\beta)/\beta\sin\beta\ , \quad \beta = \Theta/2\ . \tag{13}$$

The basic equation of motion of the film with tension/ speed control in the axial direction is written as follows:

$$T(t) = \overline{T} + M_e\ddot{z} + C_e\dot{z} + k_e z\ , \tag{14}$$

where $\overline{T}$ is a static tension applied to the film. In the present analysis, it can be written $\overline{T} = Mg$, using the mass M of the weight set at the both ends of the film, as shown in the experimental setup. M_e, C_e and K_e are equivalent mass,

Copyright © 2010 by ASME

damping and stiffness coefficients due to PID controller and structural parameters of the guide rollers and supports. In this study, the effect of the PID controller is not considered.

The axial motion of the film can be approximately expressed as follows:

$$z(t) \approx H(t)\beta = H(t)\frac{\Theta}{2}. \quad (15)$$

Stability Analysis and Instability Condition

Using steady and unsteady terms, the gap width, tension, and pressure and flow rate of air can be expressed as flows:

$$\begin{aligned} &H(t) = \overline{H} + \Delta H(t), \quad T(t) = \overline{T} + \Delta T(t), \\ &P(t) = \overline{P} + \Delta P(t), \quad P_c(t) = \overline{P}_c + \Delta P_c(t), \\ &Q(t) = \overline{Q} + \Delta Q(t), \quad \overline{Q} = Q_s, \quad V = \overline{V} = V_0. \end{aligned} \quad (16)$$

Substituting Equation (16) into the above basic equations of the air flow and the film motion, steady equations are derived

$$\begin{aligned} &\overline{T} = \alpha R \overline{P}_c, \quad 2B\overline{Q}_g = \overline{Q}, \quad \overline{Q} = Q_s, \\ &\overline{P}_c = \rho \frac{\lambda}{4} \frac{L\overline{Q}_g^2}{\overline{H}_3}, \quad \overline{P}_c = \overline{P}. \end{aligned} \quad (17)$$

From Equations (17), the equilibrium gap width $\overline{H}$, which is the floating gap of the film, is derived as follows:

$$\overline{H}^3 = \delta \frac{Q_s^2}{\overline{T}}, \quad \delta = \frac{\rho\lambda}{16} \frac{\sin\beta}{(1+\cos\beta)} \frac{R^2}{B^2}. \quad (18)$$

Unsteady equations are derived as follows:

$$\frac{\Delta P_c(t)}{\overline{P}_c} = -3\frac{\Delta H(t)}{\overline{H}} + 2\frac{\Delta Q_g(t)}{\overline{Q}_g}, \quad (19)$$

$$2B\Delta Q_g(t) = \Delta Q(t), \quad (20)$$

$$\Delta T(t) = \alpha R \Delta P_c(t), \quad (21)$$

$$\Delta T(t) = \frac{\Theta}{2}(M_e \Delta\ddot{H}(t) + C_e \Delta\dot{H}(t) + K_e \Delta H(t)), \quad (22)$$

$$\frac{\overline{V}}{K}\Delta\dot{P}(t) + \Delta Q(t) = 0, \quad (23)$$

$$\Delta P(t) = \Delta P_c(t). \quad (24)$$

Taking Laplace transform of the above unsteady Equations (19) ~ (24), the characteristic equation of the system can be obtained as follows:

$$(s^2 M_e + sC_e + K_e)\Delta\widetilde{H}(s) = \Delta\widetilde{F}(s), \quad (25)$$

$$\Delta\widetilde{F}(s) = -\frac{\varepsilon}{1+\tau s}\Delta\widetilde{H}(s), \quad (26)$$

where s indicates Laplace transform operator, and $\Delta\widetilde{H}(s)$ denotes the Laplace transformed $\Delta H(t)$. In these equations, coefficients ε and τ are given by

$$\varepsilon = \frac{3\overline{T}}{\beta\overline{H}}, \quad \tau = \frac{2\overline{P}}{Q_s}\frac{\overline{V}}{K} = \frac{2V_0}{\gamma Q_s}. \quad (27)$$

Applying Routh-Hurwitz stability criterion to Equation (25) and (26), Instability condition of the system is derived as follows:

$$C_e(1+\omega_n^2\tau^2) - \tau\varepsilon < 0. \quad (28)$$

where $\omega_n^2 = K_e / M_e$.

Discussion on the Instability Mechanism

In Equation (28), it can be found that ε and τ are very important parameters for the stability of the system. In this equation, τ indicates the effect of compressibility of the air inside the air-turn bar. Moreover, from Equations (25) and (26), it is found that τ is time constant of first-order lag element in the term of the pressure fluctuation acting on the film.

Thus, it is found that the system loses stability due to the compressibility of the air inside the air-turn bar. The system loses stability when ε becomes large, and it is led that the self-excited vibration occurs in the film when the tension is large and equilibrium gap width is small.

Assuming that the vibration displacement of the film is sinusoidal and using Equation (26), the pressure fluctuation $\Delta F(t)$ acting on the film can be obtained as follows:

$$\Delta H(t) = h\sin\omega t, \quad (29)$$

$$\Delta F(t) = \frac{\varepsilon\tau}{1+\omega^2\tau^2}\Delta\dot{H}(t) - \frac{\varepsilon}{1+\omega^2\tau^2}\Delta H(t). \quad (30)$$

The Lissajous curves of the film displacement $\Delta H(t)$ and fluid force $\Delta F(t)$ due to the pressure fluctuation acting on the film, in the case of (a) $\tau = 0$ and (b) $\tau \neq 0$, are shown in Figure 13(a) and (b). It can be seen that, when τ is zero, the pressure fluctuation has an air cushion (spring) effect, because the air force is a restoring force $\Delta F(t) = -\varepsilon\,\Delta H(t)$. On the other hand, when τ is not zero, the pressure fluctuation has not only the air cushion effect but also negative damping effect. The phase of the fluid force $\Delta F(t)$ due to the pressure fluctuation is led against the film displacement $\Delta H(t)$ and is little smaller that 180 degrees. The similar aero-dynamical characteristics of the

Copyright © 2010 by ASME

pressure fluctuation can be seen in the experimental result shown in Figure 11. These results are in a good agreement with respect to the phase relationship between the pressure fluctuation and film vibration. This result indicates the instability mechanism of the self-excited vibration generated in the film. Therefore, it is clarified that the self-excited vibration occurs, because the phase of the air pressure fluctuation is led against the film vibration due to the compressibility of the air inside the air-turn bar.

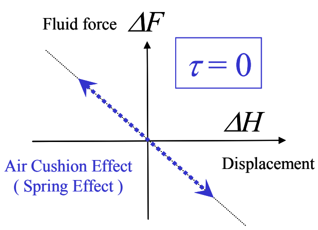

(a) In the case of $\tau = 0$

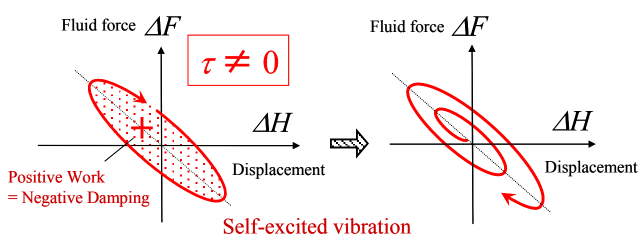

(b) In the case of $\tau \neq 0$

Figure 13 Lissajous curves of fluid force and vibration displacement of film.

Stability diagram, which denotes the instability region in which the low-frequency mode vibration occurs, as a function of the flow rate and tension is shown in Figure 14. In this figure, solid line - and ● indicates the theoretical calculation and experimental result, respectively. The stable region denotes that the low-frequency mode vibration is not excited, and the unstable region denotes that the low-frequency mode vibration is excited. In the theoretical calculations, ω_n and C_e are identified from the response of the free vibration of the film in the preliminary experiments. It can bee seen that the self-excited vibration occurs when the tension and air flow rate become larger. The theoretical calculation is in close agreement with the experimental results on the unstable region.

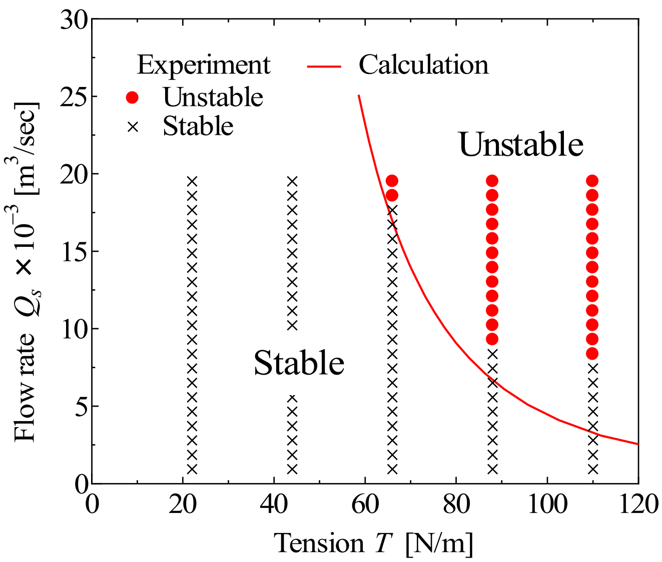

Figure 14 Stability diagram (Instability region) for the low-frequency mode vibration as a function of flow rate and tension.

CONCLUSIONS

In the present work, stability of the film wrapped around the air-turn bar has been examined theoretically and experimentally. In the experiments, vibration modes of the self-excited vibration have been clarified and the vibration characteristics have been investigated. In the theoretical analysis, the analytical model has been developed and instability condition and stability diagram have been shown by stability analysis. The major results obtained in this study are summarized as follows:

(1) Two different types of self-excited vibration, which are low-frequency and high-frequency modes, occur in the film.

(2) The self-excited vibration of the low-frequency mode occurs in the film due to the air pressure fluctuation, which is coupled with the film vibration, in the gap between the film and the air-turn bar.

(3) The self-excited vibration occurs, because the phase of the air pressure fluctuation is led against the film vibration due to the compressibility of the air inside the air-turn bar.

(4) The self-excited vibration occurs when the tension applied to the film and air flow rate become larger.

In the future work, a theoretical model for the high-frequency mode should be developed. The instability condition of not only the low-frequency mode but also height-frequency

Copyright © 2010 by ASME

mode should be clarified to avoid the damage in the film due to the vibration.

ACKNOWLEDGEMENT

This research work was supported by Japan Society for the Promotion of Science, Grant-in-Aid Scientific Research (C)-20560225. The authors are grateful to graduate students, Kazuki Uehara and Yasuharu Igarashi, for the experimental assistance.

REFERENCES

[1] Muftu, S., 2007, “Mechanics of a Thin, Tensioned Shell, Wrapped Helically around a Turn-Bar”, Journal of Fluids and Structures, **23**, pp.767-785.

[2] Muftu, S., and Cole, K. A., 1999, “The Fluid-Structure Interaction in Supporting a Thin Flexible Cylindrical Web with an Air Cushion”, Journal of Fluids and Structures, **13**, pp.681-708.

[3] Muftu, S., Lewis, T. S., Cole, K. A., and Benson, R.C., 1998, “A Two-Dimensional Model of the Fluid Dynamics of an Air Reverser”, ASME Journal of Applied Mechanics, **65**, pp.171-177.

[4] Chang, Y. B., and Moretti, P. M., 2000, “Aerodynamic Characteristics of Pressure-Pad Air Bars”, ASME Journal of Applied Mechanics, **67**, pp.177-182.

[5] Hashimoto, H., 1999, “Air Film Thickness Estimation in Web Handling Processes”, ASME Journal of Tribology, **121**, pp.50-55.

[6] Hashimoto, H., and Nakagawa, H., 2001, “Improvement of Web Spacing and Friction Characteristics by Two Types of Stationary Guides”, ASME Journal of Tribology, **123**, No.1, pp.509-516.

[7] Hashimoto, H., 1995, “Theoretical Analysis of Externally Pressurized Porous Foil Bearings–Part I: In the Case of Smooth Surface Porous Shaft”, ASME Journal of Tribology, **117**, No.1, pp.103-111.

[8] Lin, C. C., and Mote, Jr., C. D., 1995, “Equilibrium Displacement and Stress Distribution in a Two-Dimensional, Axially Moving Web under Transverse loading”, ASME Journal of Applied Mechanics, **62**, pp.772-779.

[9] Dowell, E. H., 1966, “Flutter of Infinitely Long Plates and Shells-Part I: Plate”, AIAA Journal, **4** (8), pp.1370-1377.

[10] Oyibo, G. A., 1983, “Unified Aeroelastic Flutter Theory for Very Low Aspect Ratio Panels”, AIAA Journal, **21** (11), pp.1581-1587.

[11] Chang, Y. B., and Moretti, P. M., 2002, “Flow-Induced Vibration of Free Edges of Thin Films”, Journal of Fluids and Structures, **16**, pp.989-1008.

[12] Chang, Y. B., and Moretti, P. M., 1991, “Interaction of Fluttering Webs with Surrounding Air”, TAPPI Journal, **74**, pp.231-236.

[13] Datta, S. K., and Gottenberg, W. G., 1975, “Instability of an Elastic Strip Hanging in an Airstream”, ASME Journal of Applied Mechanics, **42**, pp.195-198.

[14] Lemaitre, C., Hemon, P., and de Langre, E., 2005, “Instability of a Long Ribbon Hanging in Axial Flow”, Journal of Fluids and Structures, **20**, pp.913-925.

[15] Yamaguchi, N., Ito, K., and Ogata, M., 2003, “Flutter Limits and Behaviors of Flexible Webs Having a Simplified Basic Configuration in High-Speed Flow”, ASME Journal of Fluid Engineering, **125**, pp.345-353.

[16] Watanabe, Y., Suzuki, S., Sugihara, M, and Sueoka, Y., 2002, “An Experimental Study of Paper Flutter”, Journal of Fluids and Structures, **16**, pp.529-542.

[17] Watanabe, Y., Isogai, K., Suzuki, S., and Sugihara, M., 2002, “A Theoretical Study of Paper Flutter”, Journal of Fluids and Structures, **16**, pp.543-560.

[18] Bidkar, R. A., Raman, A., and Bajaj, A. K., 2008, “Aeroelastic Stability of Wide Webs and Narrow Ribbons in Cross Flow”, ASME Journal of Applied Mechanics, **75**, pp.041023-1~041023-9.

[19] Filippone, A., 2008, “On the Flutter and Drag Forces on Flexible Rectangular Canopies in Normal Flow”, ASME Journal of Fluids Engineering, **130**, pp.061203-1~061203-8.

[20] Guo, C. Q., and Paidoussis, M. P., 2000, “Stability of Rectangular Plates with Free Side-Edges in Two-Dimensional Inviscid Channel Flow”, ASME Journal of Applied Mechanics, **67**, pp.171-176.

[21] Tang, L., and Paidoussis, M. P., 2007, “On the Instability and the Post-Critical Behavior of Two-Dimensional Cantilevered Flexible Plates in Axial Flow”, Journal of Sound and Vibration, **305**, pp.97-115.

[22] Tang, D. M., Yamamoto, H., and Dowell, E. H., “Flutter and Limit Cycle Oscillations of Two-Dimensional Panels in Three-Dimensional Axial Flow”, Journal of Fluids and Structures, **17**, pp.225-242.

[23] Wu, X., and Kaneko, S., 2005, ”Linear and Nonlinear Analysis of Sheet Flutter Induced by Leakage Flow”, Journal of Fluids and Structures, **20**, pp.927-948.

[24] Nagakura, H., and Kaneko, S., 1992, ”The stability of a Cantilever Beam Subjected to One-Dimensional Leakage Flow,” Transaction of the JSME, **58**C (546), pp.352-359, (in Japanese).

[25] Shimoyama, Y. and Yamada, Y., “Experiments on the Labyrinth Packing, 1st Report”, Transaction of the JSME, **23**-(125), pp.44-49, (in Japanese).

 Copyright © 2010 by ASME